Journal of Materials Chemistry B

Accepted Manuscript

This article can be cited before page numbers have been issued, to do this please use: S. Soylemez, T. Yilmaz, E. Buber, Y. udum arslan, S. Ozcubukcu and L. Toppare, *J. Mater. Chem. B*, 2017, DOI: 10.1039/C7TB01674C.

ROYAL SOCIETY OF CHEMISTRY

rsc.li/materials-b

View Article Online
DOI: 10.1039/C7TB01674C

Journal Name

ARTICLE

Polymerization and biosensor application of water soluble peptide-SNS type monomer conjugates

Received 00th January 20xx,
Accepted 00th January 20xx

DOI: 10.1039/x0xx00000x

www.rsc.org/

Saniye Soylemez[a], Tuğçe Yılmaz[a], Ece Buber[a], Yasemin A. Udum[b], Salih Özçubukçu[a,c*] and Levent Toppare[a,c,d,e*]

A simple and efficient approach for the preparation of biosensing platform was developed based on newly designed peptide-SNS type monomer conjugates. The approach involves the electrochemical polymerization of the peptide-SNS type monomer on the electrode surface. To synthesize peptide bearing monomers, the SNS-type monomer having a carboxylic acid functional group was anchored to the C-terminal of peptide by solid phase peptide synthesis via coupling reagents. Utilization of peptides to increase the solubility of the monomers was first investigated with this report. The obtained monomers, soluble in water, were fully characterized by spectral analyses and utilized as matrices for biomolecule attachment. Polymerization of monomers in water has the potential to provide an alternative process for the electrochemical preparation of the polymers in aqueous medium, without using any organic solvent. Under the optimized conditions, the biosensor responded to the target analyte; glucose, with a strikingly selective and sensitive manner, and showed promising feasibility for the quantitative analysis of glucose in beverages.

Introduction

In the past few decades increasing number of people suffered from diabetes mellitus has made it a leading threat for human health. The research on accurate and sensitive detection of glucose is of great importance for early diagnosis and detection of diabetes. Biosensors are promising devices for glucose detection due to their high sensitivity, selectivity, short analysis time and low cost compare to HPLC or spectrophotometric equipments.[1] Due to their considerable advantages of great electrical, electronic and optical properties, conjugated polymers (CPs) provide a feasible alternative in designing numerous types of biosensing platforms.[2,3] In addition to providing a suitable immobilization platform for biomolecules, CPs have a tendency to enhance stability and sensitivity of the biosensors.[2,4-6] The requirement for successful enzyme loading with excessive activity motivates research into the improvement of matrices with durable and easy bioconjugation. Functionalized CPs can facilitate covalent immobilization which allows further modification with materials to improve biosensor performance. Since the choice of a suitable matrix is very important for successful detection of analyte, adapting the electrode surface to construct such a functional biosensor remains a challenge.

Peptides are an important class of molecules which cover organic and biochemical materials and as a consequence of this, they have a large variety of applications in biomaterials[7], medicinal chemistry[8], drug delivery systems[9], biosensors[10], organic electronics[11], molecular recognitions[12] etc. It is possible to attain different structures (alpha-helices, beta sheet etc.) and properties (hydrophilic, hydrophobic surfaces) just by proper selection of the amino acids. They also play a critical role in the generation of hybrid materials such as peptide-inorganic systems[13] and peptide-polymer conjugates.[14] Peptides with polar side chains such as aspartic acid, glutamic acid, and arginine are mostly soluble in water. Conjugation of the peptide having these amino acids to a poorly soluble hydrophobic molecule would enhance its solubility in water.[15] Conjugation of hydrophilic groups or even polymers such as PEG to a hydrophobic monomer to increase its water solubility is a common strategy especially in the preparation of water soluble conjugated polymers for biosensor applications.[16] Same strategy was also used to solubilize drug molecules which are very hydrophobic and poorly soluble in water.[17] Peptide-polymer conjugates are new classes of materials that are applicable to wide range of areas utilizing the features of both components to generate unique properties.[18,19] Moreover, peptides are fascinating biomaterials mimicking natural proteins[20,21] and they can show great enhancement in the solubility of the hydrophobic molecules in water and polar organic solvents. However, utilization of peptides to increase the solubility of the monomers has not been investigated to the best of our knowledge. Peptide conjugation to monomers[22,23] can also

[a] Department of Chemistry, Middle East Technical University, Ankara 06800, Turkey
[b] Department of Advanced Technologies, Gazi University, Ankara 06500, Turkey
[c] Department of Biotechnology, Middle East Technical University, Ankara 06800, Turkey
[d] Department of Polymer Science and Technology, Middle East Technical University, Ankara 06800, Turkey
[e] The Center for Solar Energy Research and Application (GUNAM), Middle East Technical University, Ankara 06800, Turkey

View Article Online
DOI: 10.1039/C7TB01674C

exhibit a good platform for the immobilization of the enzymes when the monomer is polymerized. For a biosensor design, electrogenerated film matrices provide good stability and improvements for biomolecule immobilization.[24] Furthermore, peptides on the polymer surface and enzyme molecules would show versatile interactions since they are both made of amino acids. This phenomenon may allow producing high performance biosensors and long term storage in immobilized surfaces.

Taking into consideration of the above-mentioned views, herein we report the synthesis, characterization, and biosensing application of water soluble SNS-type monomers bearing peptide side chains. Although there are several methods to conjugate peptides to polymers, covalent attachment is one of the most common ways to anchor peptides to polymers. However, it is also possible to conjugate peptides to monomers during solid phase peptide synthesis.[25] Hence in this work, firstly a SNS-type carboxylic group containing monomer was synthesized and then, two different peptides (sequences of glutamic acid-arginine-arginine (ERR) and glutamic acid-arginine-arginine (ERRR)) were anchored to a SNS-type carboxylic group containing monomer in order to increase their solubility in water. This modification allows well-organized molecular structure of the conjugated polymers on the substrates, and they constitute wonderful three dimensional matrices for the biomolecule deposition while maintaining their biological activity for a long term period. Additionally, short peptide sequence allowed easy synthesize in small quantities, making the scale up of the production of the device economically affordable. The design makes the biosensor an ideal candidate to develop a cheap device. Moreover, the corresponding monomer design was really attractive due to their functional groups as they are open to covalent bonding. Peptides are acting as linkers between polymer and glucose oxidase to generate a biocompatible medium between the enzyme and the electrode surface. To access the conjugated biopolymer architecture, the constructed monomers (SNS-COOH, SNS-ERR, and SNS-ERRR) were electrochemically polymerized on the graphite electrode via cyclic voltammetry. The electropolymerization of the monomers comprises an E(CE)n (electrochemical, chemical, electrochemical) mechanism consisting, as the first step, the formation of a radical cation.[26,27] After electropolymerization of the monomers, GOx was immobilized on these polymeric surfaces and used for glucose detection. In a subsequent step, the matrix was fixed using glutaraldehyde (GA) as the crosslinking agent. In this study, it is demonstrated that conjugated coatings based on peptide sequences in combination with glucose oxidase provide a simple route to manufacture surfaces that can act as a glucose biosensor. Scheme 1 displays the procedure to construct glucose biosensor.

Scheme 1. Schematic representation of proposed glucose biosensors.

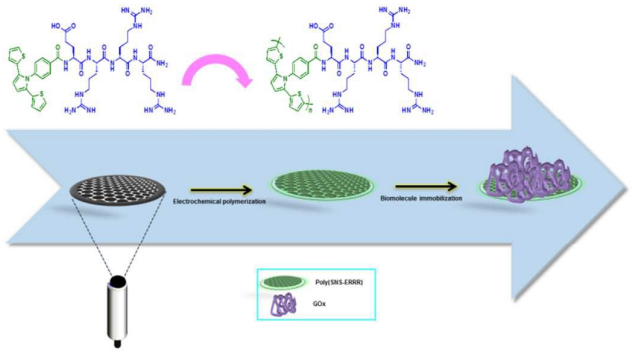

Experimental

Materials

All amino acids and reagents for peptide synthesis were obtained from Chem-Impex, IL, USA. Dimethylformamide (DMF), CH_3CN, CH_2Cl_2 and starting materials and reagents for the SNS monomer synthesis were purchased from Sigma-Aldrich. Glucose oxidase (GOx, β-D-glucose: oxygen 1-oxidoreductase, EC 1.1.3.4, 17300 units/g solid) from *A. niger* and glucose were purchased from Sigma-Aldrich. Glutaraldehyde (GA) was obtained from Sigma–Aldrich Co., LCC. (St. Louis, USA). For enzyme immobilization, a 50 mM, pH 7.0 phosphate buffer saline (PBS) solution consisting of 0.025 M Na_2HPO_4 and 0.025 M NaH_2PO_4 (Fisher Scientific Company) was used. As the substrate, glucose solution (0.1 M) was prepared by dissolving 0.18 g of glucose in 10 mL pH 7.0 PBS solution.

Measurements

Peptide synthesis was performed by the Discover Bio - Manual Microwave Peptide Synthesizer (CEM Corporation, USA). The purification of the crude peptides was performed with Dionex Ultimate 3000 Series equipped with a variable wavelength absorbance detector using a reverse phase C8 column (Hypersil Gold, 12 µm, 250 × 10 mm). A binary gradient of water (0.1% TFA) and acetonitrile (0.1% TFA) were used with a flow rate of 3.0 mL min^{-1} and the eluent was monitored by UV absorbance at 210 and 280 nm. Fractions were collected and lyophilized after their purity was confirmed by analytical HPLC performed using a RP-C18 column (Acclaim 120, 3.0 µm, 4.6 × 150 mm) with a flow rate of 0.5 mL min^{-1}.

PalmSens potentiostat (PalmSens, Houten, The Netherlands) was used for the amperometric measurements. Three electrode system containing a graphite rod (Ringsdorff Werke GmbH, Bonn, Germany, type RW001, 3.05 mm diameter and 13% porosity), a platinum wire (Metrohm, Switzerland) and a Ag wire were used as the working, counter and reference electrodes, respectively. Prior to electrochemical polymerization reaction, spectroscopic grade graphite rods were polished on an emery paper and washed thoroughly with

View Article Online
DOI: 10.1039/C7TB01674C

distilled water. For biosensor applications, electrochemical polymerizations were carried out on cleaned graphite electrodes via cyclic voltammetry using Gamry Instruments Reference 600 potentiostat/galvanostat (GAMRY Instruments Inc., Pennsylvania, USA). During electrochemical and spectroelectrochemical studies, indium tin oxide (ITO) doped glass slides were used. Spectroelectrochemical studies were performed via UV-Vis spectra (Agilent G1103A spectrophotometer). The potential for spectroelectrochemical studies was controlled using a Solatron 1285 potentiostat/galvanostat. All experiments were conducted under ambient conditions (25°C). In amperometric analyses, the data were given as the average of three measurements and standard derivations were recorded as ±SD. For surface imaging of the fabricated biosensor, scanning electron microscope (SEM) (JEOL JSM-6400 model) was used.

Synthesis of SNS-COOH and peptide anchored SNS-type monomers (SNS-ERR and SNS-ERRR)

Methyl 4-(2,5-di(thiophen-2-yl)-1*H*-pyrrol-1-yl) benzoic acid (SNS-COOH)

SNS monomer was synthesized based on a literature report in three steps starting from thiophene and succinyl chloride.[28] The first step was the Friedel Craft acylation reaction between thiophene and succinyl chloride using $AlCl_3$ at 0 °C to give diketone 1. The following step was the Paal-Knorr Pyrrole synthesis with methyl-4-aminobenzoate using pTSA as catalyst in toluene at reflux temperature under argon. As the last step, basic hydrolysis of methyl ester with LiOH in THF/MeOH mixture at room temperature gave SNS-COOH monomer 3 in good yield (26% over 3 steps) (Scheme 2). The structures of monomers were confirmed by ^{1}H NMR, IR spectroscopy, HRMS and compared with the literature results.[29]

IR (ν): 3430–3187 (br, OH), 1660 (C=O), 1510, 1417 cm^{-1} (C–S in thiophene); ^{1}H NMR ($CDCl_3$) 6.50–6.53 (m, 4H), 6.89 (dd, 2H), 7.16 (dd, 2H), 7.38 (d, 2H), 7.69 (d, 2H); MS (EI) m/z = 351 (M+, 100%); HRMS (ES+) calcd. for $C_{19}H_{13}NO_2S_2$ $[M+1]^+$ 352.0464, found 352.0458.

SNS-Peptide Conjugate (SNS-ERR (4) and SNS-ERRR (5))

To synthesize peptide moiety, solid phase peptide synthesis based on standard Fmoc chemistry was performed using Rink Amide resin under microwave conditions. 0.05 mmol resin were used and each coupling was done at 20 W and 75 °C with HBTU in DMF as the coupling agent and DIEA as the base. 5.5 fold amino acids were used for a 5 min. coupling duration. Deprotection of Fmoc group was done with 20% piperidine in DMF solution (Scheme 3).

After completing all coupling reactions of amino acids, SNS-peptide conjugation was done on resin using the same coupling condition for the amino acids. After the cleavage of side chain and resin with 95% TFA-2.5% TIPS-2.5% H_2O, SNS-COOH monomer conjugated peptide derivatives (4 and 5) have been obtained as the crude products.

The purification was done by semi-preparative RP-HPLC (Figures S3 and S4) and characterizations were performed by LC-MS and ^{1}H NMR spectroscopy to confirm the structures.

HRMS for 4; calculated: 792.3074, Found: 792.3077.

IR for 4 (ν): 3306, 3188, 3500-3000 (bs), 1647, 1532, 1501, 1414, 1180, 1045, 857, 699 cm^{-1}.

^{1}H NMR for 4 (d_6-DMSO): 8.92 (d, *J*=6.7 Hz, 1H, -N*H*-CH), 8.45 (d, *J*=6.7 Hz, 1H, -N*H*-CH), 8.06 (d, *J*=8.2 Hz, 2H), 7.42 (d, *J*=8.4 Hz, 2H), 7.31 (dd, *J*=5.0, 1.2 Hz, 2H), 7.16 (bs, 2H, -NH_2), 6.97 (bs, 2H, -NH_2), 6.89 (dd, *J*=5.3, 3.6 Hz, 2H), 6.66 (dd, *J*=3.6, 1.2 Hz, 2H), 6.59 (s, 2H), 4.45-4.52 (m, 1H, α*H*), 4.05-4.10 (m, 1H, C*H*), 3.90-3.95 (m, 1H, C*H*), 2.91-3.22 (m, 4H, -CH_2-N), 2.30-2.36 (m, 2H, -CH_2-COOH), 1.80-1.85 (m, 2H, -CH_2-), 1.49-1.66 (m, 8H, -CH_2-).

HRMS for 5; calculated: 947.4007, Found 947.4018.

IR for 5 (ν): 3281, 3194, 3500-2950 (bs), 1647, 1533, 1501, 1414, 1170, 1042, 857, 695 cm^{-1}.

^{1}H NMR for 5 (d_6-DMSO): 8.72 (d, *J*=7.2 Hz, 1H, -N*H*-CH), 8.22 (d, *J*=7.7 Hz, 1H, -N*H*-CH), 8.05 (d, *J*=7.5 Hz, 1H, -N*H*-CH), 7.99 (d, *J*=8.4 Hz, 2H), 7.93 (d, *J*=7.7 Hz, 1H, -N*H*-CH),7.49 (d, *J*=8.4 Hz, 2H), 7.33 (dd, *J*=5.1, 1.0 Hz, 2H), 7.23 (bs, 1H, -N*H*), 7.13 (bs, 2H, - NH_2), 7.10 (bs, 1H, -N*H*), 6.90 (dd, *J*=5.1, 3.6 Hz, 2H), 6.68 (dd, *J*=3.6, 1.1 Hz, 2H), 6.60 (s, 2H), 4.49-4.47 (m, 1H, α*H*), 4.24-4.30 (m, 2H, C*H*), 4.14-4.19 (m, 1H, C*H*), 3.04-3.16 (m, 6H, -CH_2-N), 2.34-2.42 (m, 2H, -CH_2-COOH), 1.64-1.74 (m, 2H, -CH_2-), 1.46-1.58 (m, 12H, -CH_2-).

^{1}H NMR and IR spectra of 4 and 5 are quite similar since there is only one extra arginine in the conjugate 5. In ^{1}H NMR spectrum of both conjugates, the peaks between 6.6 and 8.0 ppm are due to the aromatic hydrogens on the SNS moiety of the molecule. α-Hydrogens of the peptide backbones are between 3.9 and 4.5 ppm. Aliphatic hydrogens from glutamic acid and arginine residues are seen between 1.5 and 2.0 ppm as multiplets. In IR spectra of both conjugate 4 and 5, there are the characteristic C-S band around 1414 cm^{-1}, amide carbonyl bands around 1650 cm^{-1} and NH and OH bands around 3300 cm^{-1} (Figures S1 and S2).

Scheme 2. Synthesis of SNS-COOH based on the literature protocols.

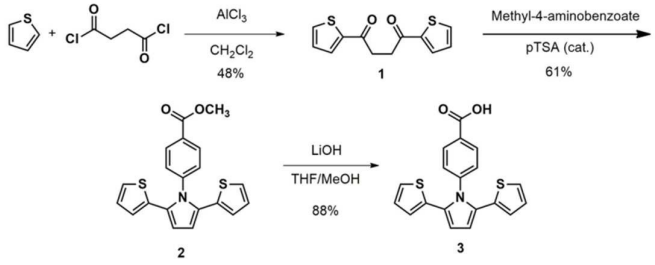

View Article Online
DOI: 10.1039/C7TB01674C

Scheme 3. Synthesis of SNS conjugated peptides 4 and 5 using standard Fmoc based solid phase peptide synthesis using Rink Amide resin.

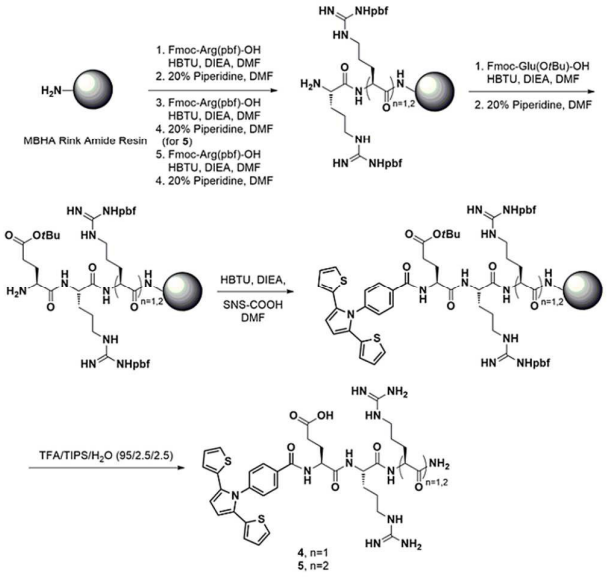

Electrochemical Biosensor Fabrication and Amperometric Measurements

Initially graphite electrodes were coated with SNS-ERRR via electrochemical deposition according to the same procedure used for biosensor preparation. Electrochemical polymerization of the monomer (SNS-ERRR) was performed in a cell containing 10^{-3} molL^{-1} of monomer, 0.1 molL^{-1} solution of $NaClO_4/LiClO_4$ (1:1) as the supporting electrolyte in the potential range between -0.3–0.5 V. Afterwards, it was used as the functional platform containing peptide handles on the surface for biomolecule deposition. For the GOx immobilization, an enzyme solution (0.75 mg in 10.0 µL, 50 mM potassium phosphate buffer, pH 7.0) was spread over the polymer coated surface. Then, 1.0 % of 5.0 µL glutaraldehyde in potassium phosphate buffer (50 mM, pH 7.0) were cast on the electrode as the cross linker, and the electrode was allowed to dry at ambient conditions for 120 min. Then, loosely bound enzyme molecules were removed by rinsing the electrode surface with the distilled water. It was stored at 4 °C when not in use. All amperometric measurements were carried out at room temperature in a reaction cell filled with 10 mL PBS, pH 7.0 under mild stirring and biosensor response signals were recorded as the current (µA) via following the oxygen consumption at −0.7 V due to the result of enzymatic activity in the bioactive surface. The calibration curves were obtained by plotting the current signal values of a series of standard glucose solution (µA) against different glucose concentrations. After the current was reached equilibrium, a certain amount of analyte solution was injected into the reaction medium, then equilibrium was established again. The difference between the two constant current values gave the biosensor response.

Results and discussion

Electrochemical and spectroelectrochemical properties of poly(SNS-ERR) and poly(SNS-ERRR)

Electrochemical Properties

Electroactivities of monomers were investigated using cyclic voltammetry technique. Cyclic voltammograms of pristine SNS-COOH monomer were obtained in ACN solution using $NaClO_4$-$LiClO_4$ (0.1 M) as the supporting electrolyte due to the poor solubility of the monomer in water. The electrochemical oxidations of SNS-ERR and SNS-ERRR were determined in a solution of $1x10^{-2}$ molL^{-1} monomer and 0.1 molL^{-1} $NaClO_4$-$LiClO_4$/H_2O electrolyte–solvent couple at a scan rate of 100 mV/s. Water solubility of the proposed monomer-peptide conjugates enable several advantages. One of the main advantages of such system is that SNS-ERR and SNS-ERRR can be easily electropolymerized in aqueous solutions that provides easy production of polymers via green chemistry. Additionally, electrodeposition could be performed at relatively low positive potentials.

Electropolymerization of SNS-COOH was performed between 0.0 V and +1.0 V in non-aqueous solution. The electroactive film was developed on the ITO surface as accompanied with an increase in the current. An irreversible oxidation peak was observed at +0.72 V referring the monomer oxidation. Upon anodic scans, polymer oxidation and reduction peaks evolved at +0.58 V and +0.30 V (Figure 1A).

In the first cycle of voltammograms shown in Figure 1B, an irreversible monomer oxidation peak for SNS-ERR was centered at +0.30 V while reversible polymer redox waves for poly(SNS-ERR) were observed at +0.25 V and +0.14 V accompanied with an increase in the current density. Since polymerization has been carried out potentiodynamically ecah run exhibits a higher current density. This is due to the electrode area increasing at every run. In Randles Sevcik equation all the parameters are fixed whereas the electrode area is increasing during polymer coating on the surface. Since the polymer itself is electroactive, this may last until all monomer is consumed. Hence the first cycle refers to the least current whilst the last one stands for the highest current. The reversible redox couple proves that electrochemical polymerization is proceeding at the ITO electrode surface to form an electroactive polymer film. An irreversible anodic wave for SNS-ERRR at +0.32 V stands for monomer oxidation (Figure 1C). Cyclic voltammetry studies indicated that SNS-ERR get oxidized at lower potentials than SNS-ERRR. Slight differences in the oxidation potentials of monomers are probably due to long chain peptide moieties in the monomer structure. During anodic scan a doping/dedoping couple was detected for poly(SNS-ERRR) as +0.23 V and +0.12 V at a scan rate of 100 mV/s.

View Article Online
DOI: 10.1039/C7TB01674C

Fig. 1. Repeated potential scan electropolymerization of **(A)** SNS-COOH in $NaClO_4$-$LiClO_4$/ACN electrolyte–solvent couple **(B)** SNS-ERR and **(C)** SNS-ERRR in 0.1 M $NaClO_4$-$LiClO_4$/H_2O electrolyte–solvent couple at a scan rate of 100 mV/s (up to 15 cycles).

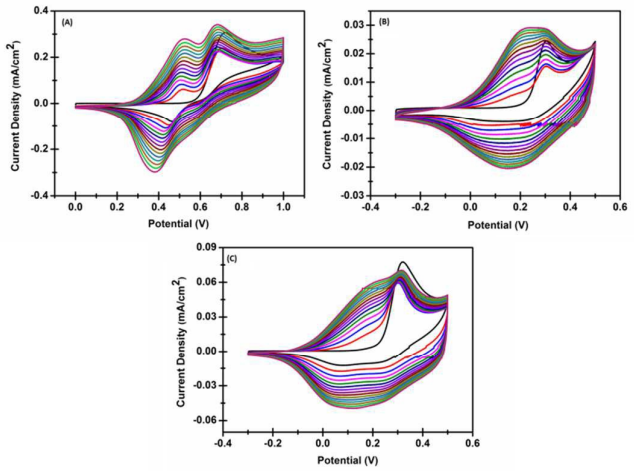

Fig. 2. Spectroelectrochemistry of **(A)** poly(SNS-ERR) and **(B)** poly(SNS-ERRR) polymer films on ITO coated glass electrodes in monomer-free 0.1 M $NaClO_4$-$LiClO_4$/H_2O at various applied potentials.

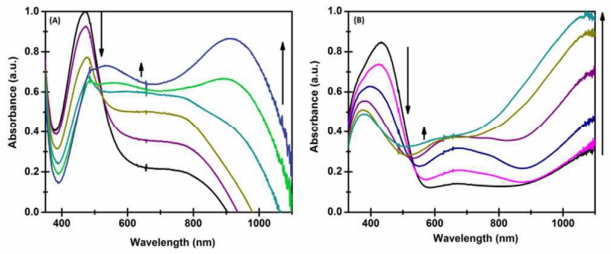

Table 1. The colors and color coordinates of conducting polymers in accordance with CIE standards.

Poly(SNS-ERR)		Poly(SNS-ERRR)		
0.0 V	0.5 V	0.0 V	0.3 V	0.5 V
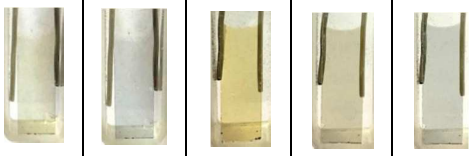				
L: 92.734 a: -10.762 b: 21.783	L: 84.602 a: -3.040 b: -1.057	L: 88.019 a: -8.261 b: 45.918	L:87.953 a: -6.259 b:18.678	L:85.681 a: -1.757 b:2.716

Spectroelectrochemistry

Spectroelectrochemical studies were carried out to determine the optical properties of poly(SNS-ERR) and poly(SNS-ERRR) upon applied potentials. For these measurements, polymer films were electrochemically deposited on ITO-coated glass plates from $1x10^{-2}$ $molL^{-1}$ monomer solution in 0.1 $molL^{-1}$ $NaClO_4$-$LiClO_4$/H_2O. Changes in optical properties of poly(SNS-ERR) and poly(SNS-ERRR) were investigated in a monomer free solution via applying increasing potentials. The newly produced electronic bands were recorded as a function of applied potential (Figure 2). The neutral state absorption maxima of poly(SNS-ERR) and poly(SNS-ERRR) were observed as wide absorptions at 470 nm and 432 nm, respectively. The maximum absorptions in the visible region can be attributed to the high energy π- π* transition of neutral state polymer.

Upon incremental stepping of the potential from 0.0 V to +0.5 V, the absorption of π- π* transitions decreases, and two new optical transitions appear at lower energy, corresponding to the polaronic and bipolaronic charge carriers. The charge carriers led to different coloration for polymer films by generating new energy transitions. As the potential increases, the absorption peaks at about 537 and 915 nm for poly(SNS-ERR) and 667 nm and 1055 nm for poly(SNS-ERRR), which correspond to polaron and bipolaron species, respectively, also increase.

Colorimetry Studies

Colorimetry studies were performed to evaluate the colors. Both polymers exhibited electrochromic properties. Poly(SNS-ERRR) reveals multi-colored electrochromic behavior with three distinct colors. The color analyses were done according to CIE 1931 Yxy color space. For the polymers color states for the pristine and oxidized forms are shown in Table 1.

Optimizations and Surface Characterization of the Biosensors

In order to obtain a proper orientation and effective binding of the enzyme on the polymer surface, optimum polymer film thickness was investigated by adjusting the cycle number during electropolymerization. The cycle number in polymerization determines the deposited charge on the polymer film, which is very much related with the thickness of the polymer layer. Stability of the enzyme on polymer film is affected by the distance between the active site of the enzyme molecule and transducer layer. Too thick polymer films hinder the electron transfer between the enzyme and the electrode causing low charge transfer rate.[30] On the other hand, thin polymer films cannot protect the enzyme from the environmental effects which may cause deformation of the matrix. To find the optimum polymer film thickness, the monomer was polymerized on a graphite electrode with different scan numbers (30, 40, 50 and 60 scans) by keeping all the other parameters constant. The highest biosensor response was obtained with 50 scans which corresponds to 39 nm (charge involved in the film formation is 25.4 mC/cm^2) in thickness (Figure S5A).

Then, the enzyme amount was optimized in order to obtain the highest biosensor response. If there is an excess loading of enzyme, the immobilized enzyme may not be fixed properly on the electrode surface since the matrix has an enzyme loading capacity. This may result in leaching out from the surface. On the other hand, if the enzyme amount is not sufficient, the

View Article Online
DOI: 10.1039/C7TB01674C

desired sensitive responses cannot be recorded.[31] In order to optimize the enzyme amount, different electrodes having 0.5 mg (8.65 U), 0.75 mg (12.98 U), 1.00 mg (17.3 U) and 1.25 mg (21.63 U) GOx were prepared. When their responses were compared, the highest signal and sufficient stability were obtained with 0.75 mg GOx (Figure S5B).

Finally, the optimum value for the pH value of the buffer solution was determined to provide an effective biosensor platform since enzyme molecules are affected by pH changes.[32] Amperometric measurements were performed using different buffer solutions in the range of pH 5.0–8.0 (sodium acetate buffer at pH 5.0, sodium phosphate buffer at pH 6.0-7.5, tris buffer at pH 8.0, 25 °C). The highest enzyme activity; therefore, the highest stable biosensor response was obtained with pH 7.0 and used for further experiments.

Cyclic voltammetry (CV) was used to investigate the charge transfer process on the biofilm surface. Effective electroactive surface areas for each surface modification were calculated using the Randless-Sevcik equation:

$Ip = 2.69 \times 10^5 AD^{1/2}n^{3/2}v^{1/2}C$

where n is the number of electrons involved in the redox reaction, A is the electrode area (cm^2), D is the diffusion coefficient of the molecule in solution ($cm^2\ s^{-1}$), C is the concentration of the probe molecule in the bulk solution (mol cm^{-3}), and v is the scan rate (V s^{-1}). According to the equation, increase in the peak currents can be attributed to an increase in effective surface area. For this purpose, cyclic voltammetry responses at bare electrode and modified electrodes were studied in a solution containing 5.0 mM $Fe(CN)_6^{3-/4-}$, 0.1 M KCl and 50.0 mM PBS pH 7.0 at the potential between 0 and 1.0 V with a scan rate of 100 mV s^{-1}. The voltammograms of different electrodes; bare graphite, poly(SNS-ERRR), and poly(SNS-ERRR)/GOx under optimum conditions were given in Figure 3. The electroactive surface areas for bare graphite, poly(SNS-ERRR) and poly(SNS-ERRR)/GOx modified electrodes were calculated as 0.072 cm^2, 0.11 cm^2 and 0.09 cm^2, respectively. In Figure 3, the poly(SNS-ERRR) modified graphite electrode had a higher peak current (121.4 µA) than the one on bare electrode (80.88 µA). This result revealed that the increase in peak current can be attributed to the increase in the effective surface area due to the generated conducting polymer film on the electrode surface. By this way, the released electrons as a result of the enzymatic reaction can be easily transferred to the transducer surface which is important for the biosensor response. After biomolecule immobilization, the decrease in the peak current confirmed the proper attachment of the biomolecule on the surface which diminished the electron transfer properties because of a possible diffusion layer. The results clearly confirm that the immobilization step for biosensor fabrication was achieved successfully.

Scanning electron microscopy (SEM) technique was used to assess the surface morphology of the modified electrodes

Fig. 3. CVs of the bare graphite electrode, poly(SNS-COOH)-coated electrode, and poly(SNS-COOH)/GOx electrode (in 5.0 mM $Fe(CN)_6^{3-/4-}$, at a scan rate of 100 mV/s)

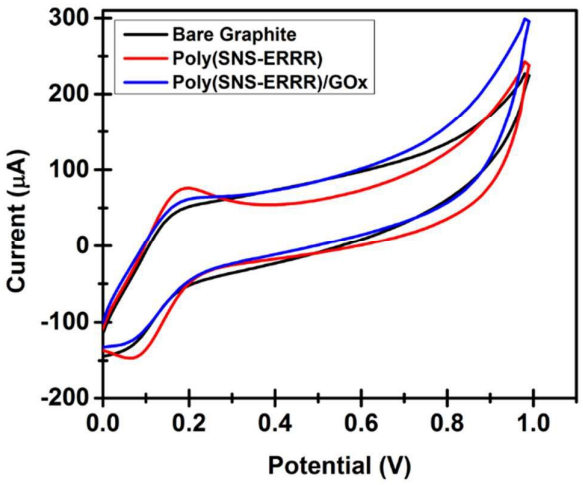

Fig. 4. SEM images showing the surface characteristics of **(A)** poly(SNS-COOH), **(B)** poly(SNS-ERR), **(C)** poly(SNS-ERRR), and **(D)** poly(SNS-ERRR)/GOx via under optimized conditions.

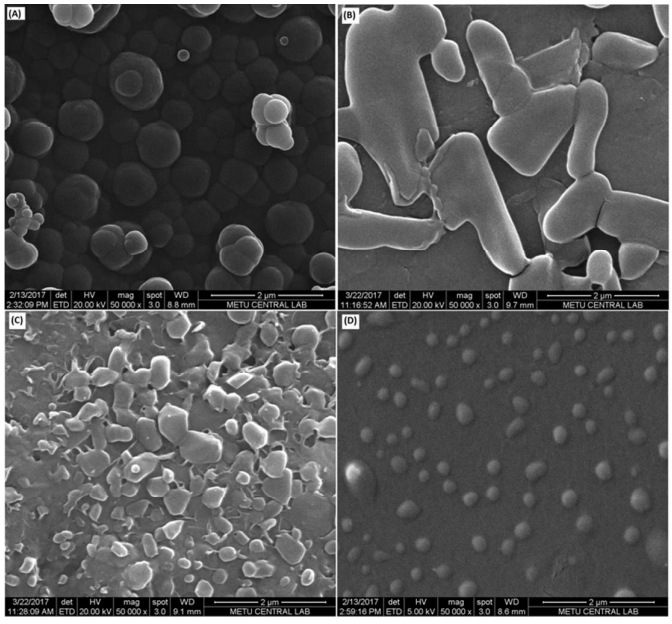

(Figures 4A-D). In the case of the typical cauliflower like structure of conjugated polymer (poly(SNS-COOH)) (Figure 4A), peptide integrated polymer surfaces (poly(SNS-ERR) and poly(SNS-ERRR)) showed completely different surface morphologies ((Figures 4B-C). A homogenous film observed on the graphite surface in the case of the combination of biolayer with the poly(SNS-ERRR) provided more ordered like structure (Figure 4D). This ordered structure allows to get more reliable

View Article Online
DOI: 10.1039/C7TB01674C

and stable biosensor responses that was proved by the analytical results.

Analytical Characterization of the Biosensors

Amperometric responses of the biosensor were recorded by adding different concentrations of glucose to buffer solution. The characteristic calibration curves for glucose were plotted and responses of biosensors were shown in Figure 5. Linear ranges for each biosensor were determined as 0.1–0.5 mM for the poly(SNS-COOH)/GOx and the poly(SNS-ERR)/GOx and 0.01-0.75 mM for poly(SNS-ERRR)/GOx modified electrodes with the correlation coefficients of 0.984, 0.997 and 0.998, respectively. Sensitivity values of the biosensors were also calculated as 19.62 μAmM^{-1} cm^{-2} for the poly(SNS-COOH)/GOx, 42.0 μAmM^{-1} cm^{-2} for the poly(SNS-ERR)/GOx and 91.37 μAmM^{-1} cm^{-2} poly(SNS-ERRR)/GOx, respectively. Poly(SNS-ERRR) modified biosensor showed the best results among the three biosensors as given with the equation; $y = 6.2875x + 0.0571$ (R^2= 0.998). For optimum biosensor, the limit of detection (LOD) value was calculated by setting the intercept of the linear range of the calibration curve to zero using S/N (signal-to-noise ratio) = 3 criterions as 4.69 µM. When compared to other modifications, this biosensor showed also very low limit of detection (LOD) value (92.7 µM for poly(SNS-COOH) and 72.14 µM for poly(SNS-ERR) modified electrode). The results revealed that the poly(SNS-ERRR) modified biosensor yields enhanced stability and affinity towards the substrate than to that of the other modifications. Furthermore, this modification displays that enzyme molecules were anchored more precisely and well-oriented, and hence, the analytical parameters were turned out to be better. Additionally, the biosensor has a rapid and sensitive response to glucose and reaches a steady-state equilibrium current in 2 s that allows easy detection of glucose in samples.

Kinetic parameters of the proposed biosensor were investigated using Lineweaver–Burk plot (1/I vs 1/[S]) at constant temperature and pH 7.0 and are listed in Table 2 comparatively with literature results. From the Lineweaver-Burk plot, K_M^{app} value was calculated as 0.208 mM. K_M shows the affinity of the enzyme molecules to their substrate. When compared to other studies in the literature, the present biosensor showed a considerably low LOD, high sensitivity and low K_M^{app} values. Liu et al proposed a glucose biosensor based on water-dispersible chitosan-functionalized graphene (CG) and further modified it with Fe_3O_4.[33] The proposed biosensor has a sensitivity value of 5.658 $\mu AmM^{-1}cm^{-2}$ with a detection limit of 16 µM. In another study, a biosensor was developed for the detection of glucose with an electrode modification of PdNPs-electrochemically reduced graphene oxide.[34] The biosensor has the Michaelis constant of 5.44 mM. Adronov et al designed a biosensor by entrapping glucose oxidase within the poly[3-(3-*N*,*N*-diethylaminopropoxy)thiophene] and single-walled carbon nanotubes films and they obtained the K_M^{app} value of 3.4 mM.[35] Moreover, a glucose biosensor utilizing polyaniline and chitosan-coupled carbon nanotubes was fabricated by Kang et al.[36] This biosensor construction showed K_M^{app} value of 5.35 mM and the sensitivity value of 21 $\mu AmM^{-1}cm^{-2}$. Another glucose biosensor based on the glucose oxidase/one-dimensional hierarchically structured TiO_2 modified electrode proposed the sensitivity of 9.9 $\mu A\ mM^{-1}cm^{-2}$ and the K_M^{app} value of 1.54 mM.[37] Poly(SNS-ERRR) matrices exhibited higher affinity toward the glucose substrate; hence, the designed biosensor served our purposes perfectly. Furthermore, a glucose oxidase biosensor prepared with methyl viologen-mediated, as the redox mediator, and glutaraldehyde (GA) crosslinker in the presence of bovine serum albumin (BSA) as carrier protein gives LOD as 20 µM.[38] In an another example, based on glucose oxidase immobilized by glutaraldehyde co-crosslinking with bovine serum albumin and Nafion® cation-exchange polymer, on a cobalt(II) phthalocyanine–cobalt(II) tetra(5-phenoxy-10,15,20-triphenylporphyrin), ($CoPc–(CoTPP)_4$) pentamer film modified glassy carbon electrode (GCE), the LOD was found as 10 µM.[39] These results also confirm the proper surface design in the present study to achieve a very low LOD without any need for membrane, redox mediator or carrier protein. The designed peptide-modified conjugated polymer layer shows both mediator and carrier property for enzymatic reactions and immobilization, respectively. This is one of the main advantages of the sensing platform for real-time applications. Other advantages of the system are its easy preparation (not requiring a multi-step preparation) and a fast response time. When compared to other modifications summarized in Table 2, the response time of our biosensor was also shortened by the help of surface orientation of the enzyme molecules. This easy preparation procedure is easy to apply, simple and effective for detection of glucose. A detailed comparison of the properties of the biosensor is summarized in Table 2.

Fig. 5. Calibration curve for glucose (in 50 mM phosphate buffer, pH 7.0, 25 °C). Error bars show standard deviation of three measurements.

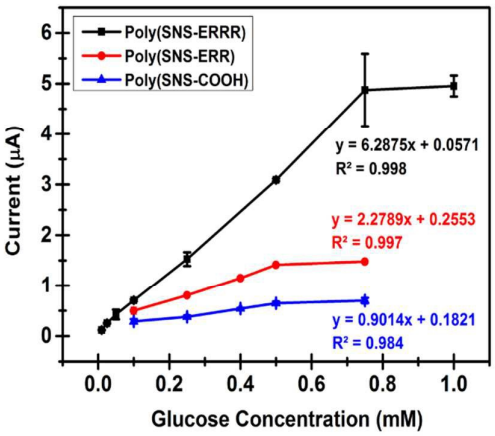

View Article Online
DOI: 10.1039/C7TB01674C

Table 2. Comparison of the various glucose biosensors for the detection of glucose

Matrices on electrodes	LOD (μM)	Sensitivity ($\mu AmM^{-1}cm^{-2}$)	K_M^{app} (mM)	References
Poly(SNS-ERRR)/GOx	**4.69**	**91.37**	**0.208**	**This work**
GOx/Au/MXene/Nafion/GCE	5.9	4.2	NR	40
Graphene–AuNPs–GOD	35	NR	4.73	41
Au cypress/PB grid	NR	74.3	1.48	42
PA-g-PEG/GOx/graphite	20	47.72	0.97	43
Poly(SNS-anchored carboxylic acid) /PAMAM-G4	2.92	NR	1.59	44
GOD/graphitic-nanocage modified GCE	8	13.3	NR	45
BNNTs-PaniPt-GOD	6	19.02	3.4	46
PET/VACNTs-Al-foil/PFLA/GOx	7.035	65.816	0.193	47
$(PAH/CdTe)_{12}(PAH/PSS)_3(PAH/GOD)_3$	500	NR	8	48
GOx/MWCNTs/CS/GCE	10	13	2.2	49
GOD/Pt/OMC/Au	50	12	NR	50

NR: Not reported

Other analytical parameters such as repeatability and shelf-life of the biosensor were also evaluated. Shelf life of the biosensor was measured by recording the biosensor responses for 0.5 mM glucose during 31 days. In a period of 31 days, there was only 5.0% decrease in the biosensor response. When not in use, the biosensor was kept at 4◦C. The device was still active with 95% efficiency after a month (Figure 6A). Additionally, the operational performance of poly(SNS-ERRR)/GOx was investigated for 20 successive measurements (with a standard deviation of 0.034% and relative standard deviation of 4.01%). The stability of the biosensor for repetitive uses in that period is quite good. Furthermore, the investigation of the biosensor selectivity toward possible interfering substances is a mandatory step in the development of biosensors. Hence, some potential interferents like ascorbic acid and urea (0.5 mM) were injected to the reaction cell instead of glucose as the substrate. The biosensor responses were followed and shown in Figure 6B. No responses were recorded for these interferents at -0.7 V potential under the optimized conditions that proves the biosensor can be comfortably used for the glucose determinations in various applications even within an environment with such interferents.

Sample Application

To test the convenience of the biosensor glucose content in several beverages were determined. For this purpose, the samples were injected into the cell instead of the glucose substrate without any pretreatment. Each sample (around 10 μL) was injected into 10 mL of buffer containing cell and an automatic dilution occurs. By this way, the detected glucose amounts were in the range of our detected linear range. The responses of the biosensor were recorded for each sample and glucose contents were estimated from the calibration curve. All these experiments were achieved under the optimum conditions. Percent relative error was calculated and the biosensor results were compared with those given on the labels provided by the manufacturers. The measurements were carried out at ambient conditions (25 °C). The proposed biosensor design is suitable for use in real time analysis to investigate glucose content in beverages. The obtained results are summarized in Table 3.

Fig. 6. (A) Shelf-life analysis of the biosensor during 31 days and **(B)** biosensor responses to glucose and interfering substances (in 50 mM phosphate buffer, pH 7.0, 25 °C).

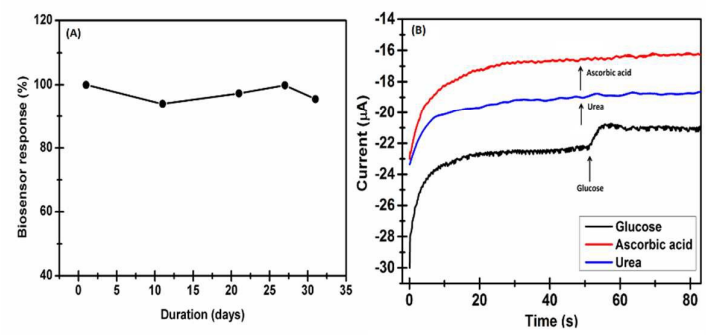

Table 3. Results of glucose analyses in beverages.

Sample	Glucose Content (mM)		Relative Error (%)
	Product Label	poly(SNS-ERRR)/GOx biosensor	
S® Ice tea	0.37	0.35 ± 0.10	5.41
S® Milk	0.25	0.23 ± 0.01	8.0
C® Coke	0.62	0.59± 0.11	4.83

View Article Online
DOI: 10.1039/C7TB01674C

Conclusions

Two new water-soluble monomers were designed and successfully synthesized by solid phase peptide synthesis via coupling reagents. The monomers were structurally characterized using ^{1}H, ^{13}C NMR and FTIR spectroscopy and HRMS to confirm the structures. The purifications of the monomers were done by semi-preparative RP-HPLC. Peptide-SNS-type monomer conjugation allowed green chemistry to achieve electropolymerization in aqueous medium. Moreover, the proposed monomers were electrochemically polymerized on graphite electrode via cyclic voltammetry and their biosensor results were evaluated using important parameters which are good indicators a for biosensor performance. Moreover, the surface characteristics of the electrodes were investigated using SEM and CV techniques. The optimum biosensor exhibited good analytical characteristics: linear range of 0.01−0.75 mmolL^{-1} (R^2 = 0.998), sensitivity 91.37 µA$mM^{-1}cm^{-2}$, and K_M^{app} 0.208 mmol L^{-1}. In virtue of the good biocompatibility and remarkable interaction of the anchored peptides with enzymes, the biosensor showed high sensitivity and favorable selectivity, and was also efficient enough to detect glucose in beverages, indicating feasible potential for practical application. Furthermore, the proposed sensing system showed a good shelf-life stability of 31 days with a very stable and reproducible results.

References

1 I. S. Kucherenko, D. Y. Didukh, O. O. Soldatkin and A. P. Soldatkin, *Anal. Chem.*, 2014, **86**, 5455.
2 T. Ahuja, I. A. Mir, D. Kumar and Rajesh, *Biomaterials*, 2007, **28**, 791.
3 S. Tuncagil, D. Odaci, E. Yildiz, S. Timur and L. Toppare, *Sens. Actuators B-Chem.*, 2009, **137**, 42.
4 D. D. Borole, U. R. Kapadi, P. P. Mahulikar and D. G. Hundiwale, *Des. Monomers Polym.*, 2006, **9**, 1.
5 B. D. Malhotra, A. Chaubey and S. P. Singh, *Anal. Chim. Acta*, 2006, **578**, 59.
6 A. K. Sarma, P. Vatsyayan, P. Goswami and S. D. Minteer, *Biosens. Bioelectron.*, 2009, **8**, 2313.
7 (a) S. Wong, M. S. Shim and Y. J. Kwon, *J. Mater. Chem. B*, 2014, **2**, 595. (b) X. Zhao, F. Pan, H. Xu, M. Yaseen, H. Shan, C. A. E. Hauser, S. Zhangcd and J. R. Luab, *Chem. Soc. Rev.*, 2010, **39**, 3480.
8 K. J. Jensen, *Peptide and Protein Design for Biopharmaceutical Applications*, John Wiley & Sons Ltd., 2009.
9 B. J. Bruno, G. D. Miller and C. S. Lim, *Ther Deliv.*, 2013, **4**, 11, 1443.
10 Q. Liu, J. Wang and B. J. Boyd, *Talanta*, 2015, **136**, 114.
11 H. A. M. Ardonn and J. D. Tovar, *Bioconjugate Chem.,* 2015, **26**, 2290.
12 T. Sawada, H. Mihara and T. Serizawa, *Chem. Rec.*, 2013, **13**, 172.
13 (a) I. M. Rio-Echevarria, R. Tavano, V. Causin, E. Papini, F. Mancin and A. Moretto, *J. Am. Chem. Soc.*, 2011, **133**, 1. (b) J.M. Swiecicki, J. Tailhades, E. Lepeltier, G. Chassainga, S. Lavielle and C. Mansuya, *Colloids and Surfaces A: Physicochem. Eng. Aspects*, 2013, **431**, 73. (c) I. M. Rio-Echevarria, R. Tavano, V. Causin, E. Papini, F. Mancin and A. Moretto, *J. Am. Chem. Soc.*, 2011, **133**, 8.
14 C. Alemán, A. Bianco and M. Venanzi, *Peptide materials: From nanostuctures to applications*, John Wiley & Sons. (Eds.), 2013.
15 A. D. Meyers, *Proteins. From analytics to structural genomics*, John Wiley & Sons. (Eds.), 2007.
16 C. Zhu, L. Liu, Q. Yang, F. Lv and S. Wang, *Chem. Rev.*, 2012, **112**, 4687.
17 T. R. M. Tan, K. M. Hoi, P. Zhang and S. K. Ng, *PloS One*, 2016, **11**, e0152112.
18 J. Y. Shu, B. Panganiban and T. Xu, *Annu. Rev. Phys. Chem.*, 2013, **64**, 631.
19 H. A. Klok, *Macromol.*, 2009, **42**, 7990.
20 J. Ling, H. Peng and Z. Shen, *J. Polym. Sci., Part A: Polym. Chem.*, 2012, **50**, 3743.
21 R. Obeid and C. Scholz, *Biomacromolecules*, 2011, **12**, 3797.
22 T. K. Paira, S. Banerjee, M. Raula, A. Kotal, S. Si and T. K. Mandal, *Macromol.*, 2010, **43**, 4050.
23 H. Murata, F. Sanda and T. Endo, *Macromol.*, 1997, **30**, 2902.
24 S. D. Uzun, N. A. Unlu, M. Sendur, F. E. Kanik, S. Timur and L. Toppare, *Colloids Surf. B*, 2013, **112**, 74.
25 T. Trimaille, K. Mabrouk, V. Monnier, L. Charles, D. Bertin and D. Gigmes, *Macromol.*, 2010, **43**, 4864.
26 P. Hapiot, P. Audebert, K. Monnier, J. Pernautt and P. Garcia, *Chem. Mater.*, 1994, **6**, 1549.
27 P. Audebert, J. Catel, G. Coustumer, V. Duchenet and P. Hapiot, *J. Phys. Chem.*, 1995, **99**, 11923.
28 F. Ekiz, F. Oğuzkaya, M. Akin, S. Timur, C. Tanyeli and L. Toppare, *J. Mat. Chem.*, 2011, **21**, 12337.
29 Y. H. Kim, J. Hwang, J. I. Son and Y. B. Shim, *Syn. Met.*, 2010, **160**, 413.
30 S. Soylemez, F. E. Kanik, M. Ileri, S. O. Hacioglu and L. Toppare, *Talanta*, 2014, **118**, 84.
31 S. Soylemez, F. E. Kanik, S.D.Uzun, S.O.Hacioglu, and L. Toppare, *J. Mater. Chem B*, 2014, **2**, 511.
32 I. H. Segel, *Enzyme kinetics: behavior and analysis of rapid equilibrium and steady state enzyme systems*, New York: Wiley, 1975.
33 W. Zhang, X. Li, R. Zou, H. Wu, H. Shi, S. Yu and Y. Liu, *Sci. Rep.*, 2015, **5**, 11129.
34 Y. Qin, Y. Kong, Y. Xu, F. Chu, Y. Tao and S. Li, *J. Mater. Chem.*, 2012, **22**, 24821.
35 X. Pang, P. Imin, I. Zhitomirsky and A. Adronov, *Macromol.*, 2010, **43**, 10376.
36 D. Wan, S. Yuan, G. L. Li, K. G. Neoh and E. T. Kang, *ACS Appl. Mater. Interfaces*, 2010, **2**, 3083.
37 P. Si, S. Ding, J. Yuan, X. W. (David). Lou and D. H. Kim, *ACS Nano*, 2011, **5**, 7617.
38 M. E. Ghica and C. M. Brett, *Anal. Chim. Acta*, 2005, **532**, 145.
39 K. I. Ozoemena and T. Nyokong, *Electrochim. Acta*, 2006, **51**, 5131.
40 R. B. Rakhi, P. Nayak, C. Xia and H. A. Alshareef, *Sci. Rep.*, 2016, **6**, 36422.
41 Y. Chen, Y. Li, D. Sun, D. Tian, J. Zhang and J. J. Zhu, *J. Mater. Chem.*, 2011, **21**, 7604.
42 Z. Chu, L. Shi, L. Liu, Y. Liu and W. Jin, *J. Mater. Chem.*, 2012, **22**, 21917.
43 T. C. Bicak, M. Gicevičius, T. C. Gokoglan, G. Yilmaz, A. Ramanavicius, L. Toppare and Y. Yagci, *Macromol.*, 2017, **50**, 1824.
44 S. Demirci, F. B. Emre, F. Ekiz, F. Oğuzkaya, S. Timur, C. Tanyeli and L. Toppare, *Analyst*, 2012, **137**, 4254.
45 C. X. Guo, Z. M. Sheng, Y. Q, Shen, Z. L. Dong and C. M. Li, *ACS Appl. Mater. Interfaces*, 2010, **2**, 2481.
46 J. Wu and L. Yin, *ACS Appl. Mater. Interfaces*, 2011, **3**, 4354.
47 T. C. Gokoglan, S. Soylemez, M. Kesik, I. B. Dogru, O. Turel, R. Yuksel, H. E. Unalan and L. Toppare, *Food Chem.*, 2017, **220**, 299.

View Article Online
DOI: 10.1039/C7TB01674C

48 X. Li, Y. Zhou, Z. Zheng, X. Yue, Z. Dai, S. Liu and Z. Tang, *Langmuir*, 2009, **25**, 6580.
49 S. Deng, G. Jian, J. Lei, Z. Hu and H. Ju, *Biosens. Bioelectron.*, 2009, **25**, 373.
50 L. D. Zhu, X. Y. Jiang, Y. H. Wu, X. Y. Mao and X. J. Cui, *Sens. Actuat. B-Chem.*, 2011, **153**, 158.